



## Research paper

# Mechanical characteristics of twin tunnel underneath construction on existing high-speed railway tunnel

Ruizhen Fei<sup>1</sup>, Limin Peng<sup>2</sup>, Chunlei Zhang<sup>3</sup>,  
Jiqing Zhang<sup>4</sup>, Peng Zhang<sup>5</sup>

**Abstract:** The running speed of high-speed trains in the tunnel is as high as 350 km, which is very sensitive to the construction disturbance of the new shield tunnel. Therefore, it is of positive significance to study the influence of shield tunneling on existing high-speed railway lines and tunnel structures and control standards. Combined with centrifuge test and three-dimensional numerical simulation, the dynamic response of shield tunnel undercrossing existing high-speed railway tunnel is studied, and the influence of settlement joint and steel pipe pile reinforcement on existing tunnel is analyzed. Studies have shown that the existence of existing tunnels will reduce the surface settlement caused by tunnel excavation, but this shielding effect will be reduced if the influence of construction joints is considered. Therefore, if the construction joint is not considered in the numerical calculation, the ground deformation will be underestimated and the mechanical performance of the existing tunnel structure will be overestimated. In addition, steel pipe piles can effectively control the settlement of existing tunnels.

**Keywords:** high speed railway tunnel, shield twin-tunnel, construction joint, ground settlement, lining stress

<sup>1</sup>PhD., Eng., Central South University, School of Civil Engineering, Changsha, 410075, China; China Railway Design Corporation, Tianjin, 300142, China, e-mail: [fruiizhen@163.com](mailto:fruiizhen@163.com), ORCID: 0000-0002-9142-4890

<sup>2</sup>Prof, PhD., Central South University, School of Civil Engineering, Changsha, 410075, China, e-mail: [limpeng@mail.csu.edu.cn](mailto:limpeng@mail.csu.edu.cn), ORCID: 0000-0002-0402-2368

<sup>3</sup>MSc., Eng., China Railway Design Corporation, Tianjin, 300142, China, e-mail: [zhangchunlei@crdc.com](mailto:zhangchunlei@crdc.com), ORCID: 0000-0002-0630-1467

<sup>4</sup>MSc., Eng., China Railway Design Corporation, Tianjin, 300142, China, e-mail: [zhangjiqing@crdc.com](mailto:zhangjiqing@crdc.com), ORCID: 0000-0002-0864-9934

<sup>5</sup>MSc., Eng., China Railway Design Corporation, Tianjin, 300142, China, e-mail: [zhangpeng04@crdc.com](mailto:zhangpeng04@crdc.com), ORCID: 0000-0001-6185-2379

## 1. Introduction

With the development of economy and the progress of society, the tunnel has been widely promoted as a construction that can shorten the distance and avoid large ramps and effectively save space on the ground [1–3]. In the construction of urban underground transportation network, the construction of new tunnels underneath existing tunnels is gradually increasing. Considering that the existing tunnel construction has changed the stress state of the original soil, for the shield tunneling project, the soil is not only affected by the construction disturbance of a single new shield tunnel, but also under the overlapping influence of the existing tunnel and the new tunnel, resulting in the complex and difficult to predict the change of the surface displacement (vertical settlement and horizontal displacement). Therefore, the influence of shield tunneling on the surface displacement has become a key issue in such engineering research [4–7].

The interaction between tunnel and soil is usually studied by field monitoring, numerical simulation and model test. On-site monitoring of tunnel physical and mechanical behavior by collecting data from sensors [8–10], but this method is time consuming, clumsy and occasionally damaging sensors. Numerical simulation of soil properties, subway tunnels, adjacent structures and their interactions [11–16], although some simplifications are needed in the calculation process, this method is efficient in calculating large-scale engineering problems. Centrifuge tests were performed to analyze tunnels with different depths, but simplified consideration was often given to complex strata or detail structures during tests [17–23].

In summary, most of the existing studies focus on the influence of new shield tunnels on existing subway tunnels or only on the influence of shield construction disturbance on surface subsidence, but there are few studies on the influence of high-speed railway tunnels under the combined action of new tunnel disturbance and existing tunnel influence. However, the operation speed of high-speed railway tunnels is as high as 350 km/h, and the deformation of existing tunnels caused by new tunnel construction may reduce the smoothness and safety of high-speed railway operation. Unlike circular subway tunnels, the section of high-speed railway tunnels is usually horseshoe-shaped, which makes the stress or deformation distribution of lining more complex. The lining of high-speed railway tunnel is constructed by construction joints along the longitudinal direction. In theoretical or numerical analysis, the lining is usually simplified as a continuous structure [24]. This kind of underground continuous beam has the effect of reducing the surface deformation caused by tunnel excavation, which is usually considered as a shielding effect [22]. However, if the high-speed railway tunnel is simplified as a longitudinal beam, it is unclear how the tunnel construction connection affects its shielding effect during tunnel excavation.

In this paper, the influence of shield tunnel under existing high-speed railway tunnel is studied by centrifuge test and three-dimensional numerical simulation. The influence of settlement joint on existing structure is studied by scale model test, and the influence of steel pipe pile reinforcement on existing high-speed railway tunnel is considered in the process of numerical calculation. The surface deformation, deformation and stress laws of

existing tunnel lining in double-tunnel construction are mainly studied, so as to provide reference for tunnel design and construction in the future.

## 2. Project profile

### 2.1. The description of project

The section of Changsha Metro Line 3 Gas Trade Avenue Station-Xing sha Avenue Station is arranged along the east-west direction of Kaiyuan West Road. The section is constructed by shield method. The shield tunnel passes through the existing high-speed railway tunnel at DK 34 + 856, which is vertical to each other, as shown in Fig. 1.

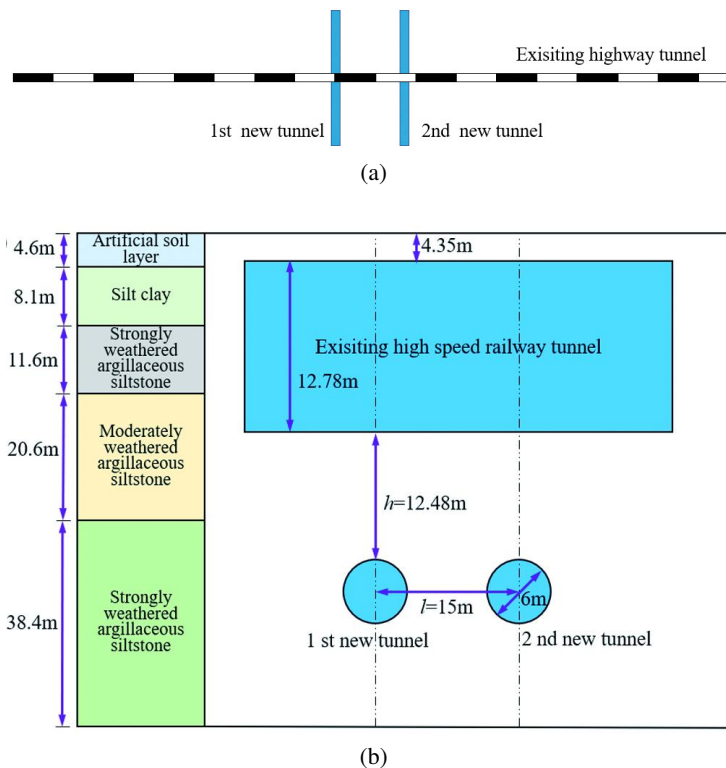


Fig. 1. Relative position relationship between existing tunnel and new tunnel:  
 (a) Plane position relation; (b) Section position relation

The high-speed railway tunnel has been put into use. Although the design speed in the tunnel is 350 km, the running speed of the high-speed train is usually 300 km. The existing tunnel lining adopts horseshoe section, the section width is 14.9 m, the height is 12.78 m,

and the inverted arch thickness is 0.9 m, as shown in Fig. 2a. The inner diameter of the newly-built shield tunnel is 5.4 m, and the outer diameter is 6.0 m. The lining is made of 0.3 m thick C50 reinforced concrete, as shown in Fig. 2b.

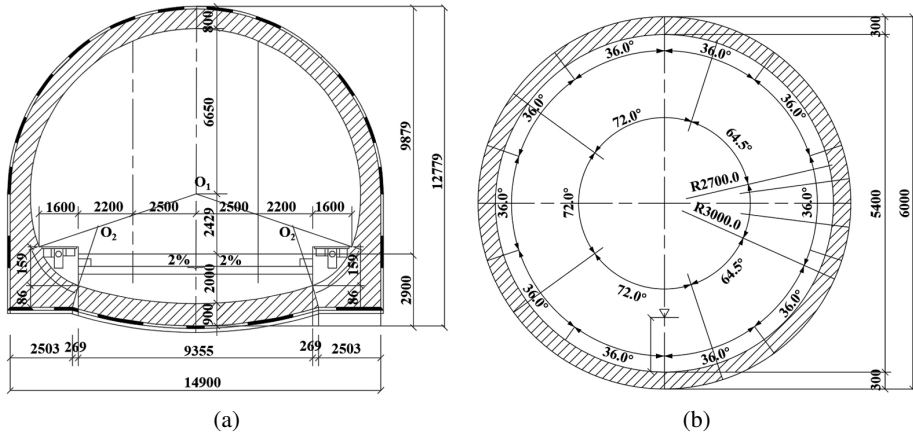


Fig. 2. Tunnel section design: (a) High-speed railway tunnel design section; (b) Design section of shield tunnel

## 2.2. Engineering geological condition

The typical soil profile in the study area is shown in Fig. 1. The upper layer is an artificial filling soil layer with a depth of 4.6 m. The underlying soil layer is characterized by silty clay with a depth of 8.1 m, followed by strong weathered argillaceous siltstone with a thickness of 3.5 m. The excavation of a new double shield tunnel underneath the weathered argillaceous siltstone is shown in Fig. 1. According to geological exploration reports, the physical and mechanical properties of each soil layer are listed in Table 1.

Table 1. Physical and mechanical properties of soil layers

Stratum	Soil unit weight (kN/m <sup>3</sup> )	Young modulus (MPa)	Inter friction angle (°)	Cohesive stress (kPa)	Poisson ratio
Artificial soil layer	19.4	10	15.0	35	0.35
Silty clay	20.0	30	16.5	42	0.3
Strongly weathered argillaceous siltstone	22.2	400	17	50	0.27
Moderately weathered argillaceous siltstone	23.0	1000	20	80	0.25

### 3. Three-dimensional centrifuge model tests

#### 3.1. Experimental program and setup

In this study, two centrifuge model tests were carried out in the centrifuge test device. The centrifuge capacity was 400 g-t, and the rotation radius was 4.2 m. These two centrifuge tests were carried out under 60 g (gravity acceleration). The model container used in the test was 1250 mm long, 930 mm wide, and 850 mm high. Except that in Test 2, a settlement joint was set on the existing tunnel, the structures of the two tests were completely the same. Fig. 3a shows the typical plane diagram of the centrifuge model. The new shield tunnel is vertical to the existing tunnel, and the left tunnel is excavated first, and the right tunnel is excavated later.

Figures 3b shows the typical elevation view of the centrifuge model. The thickness of sand is 800 mm, equivalent to 48 m of the prototype. The buried depths of the built tunnel and the newly excavated tunnel are 72.5 mm and 477.5 mm, respectively, corresponding to 4.35 m and 28.65 m in the field. The section heights of the existing tunnel and the newly excavated tunnel are 184.6 mm and 100 mm, respectively, corresponding to 11.1 m and 6 m on site.

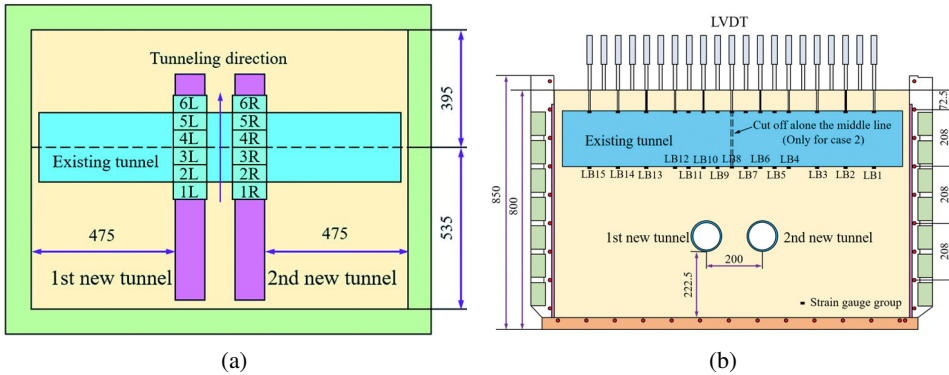


Fig. 3. Typical plan and elevation view of centrifuge model: (a) Plan view; (b) Elevation view

#### 3.2. Model tunnel settlement joint

Figure 4 shows the process of preparing the settlement joint in test 2. The existing tunnel was completely cut off at the middle line. Before the experiment, the two tunnels were temporarily connected by four thin aluminum sheets to facilitate putting them into the model box. Four potentiometers were arranged at the middle line position of the internal section of the existing tunnel to measure the change of the inner diameter of the existing tunnel in the vertical and horizontal directions.

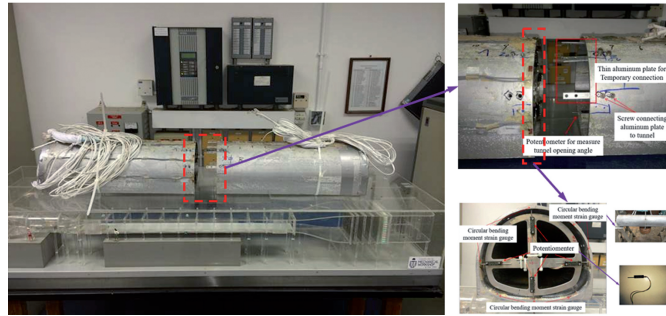


Fig. 4. Preparation process of the settlement joint

### 3.3. Simulation of tunnel excavation

In the actual construction process, shield tunnel construction is composed of earthwork excavation, tunnel lining installation and tail hole grouting. All these construction activities cause surface subsidence, but it cannot distinguish the contribution of each process to surface subsidence and existing tunnel deformation. Therefore, the overall tunnel volume loss is simulated in centrifuge test rather than detailed construction activities. In this study, in general, the simulation method of tunnel volume loss is realized by discharging a large amount of heavy liquid during the construction process, which is a common tunnel excavation simulation technology in the literature. Although this simulation technology cannot capture all tunnel construction activities, the key influence of volume loss is well captured.

As shown in Fig. 5, the model tunnel is composed of rubber bag, dumbbell-shaped frame and six drainage holes.

The outer diameter and arm thickness of the rubber film are 100 mm and 1 mm, respectively. This rubber is sealed at both ends of the dumbbell-shaped frame. Two holes

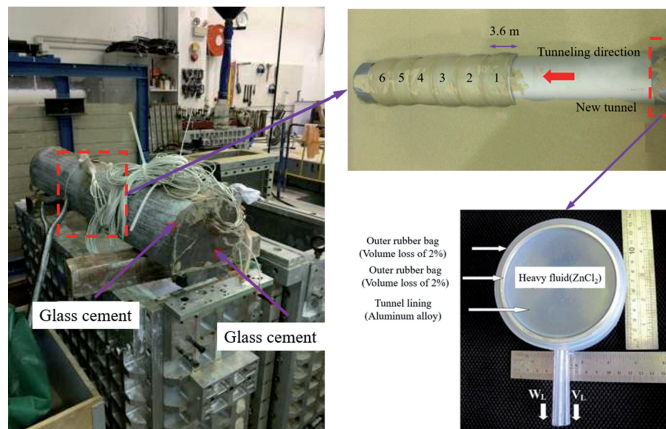


Fig. 5. Simulation system test diagram of formation loss

were designed at both ends of the dumbbell-shaped frame to remove any bubbles in the model tunnel. The two holes are sealed after removing the bubbles in the model tunnel. The rubber belt is filled with zinc chloride solution. The solution is approximately incompressible, and the density is close to that of sand in the test. In centrifuge test, the simulation of tunnel excavation is realized by releasing zinc chloride solution in one rubber bag inside and outside the tunnel lining. By releasing the solution outside the tunnel lining, the ground loss caused by tunnel excavation can be simulated (2%). The self-weight loss in tunnel can be simulated by releasing the solution in tunnel lining. Ng conducted a three-dimensional centrifuge test on the interaction between two tunnels, and found that the weight loss of the tunnel response caused by the excavation below the tunnel is negligible [19]. For convenience, tunnel volume loss is simulated by drainage during construction.

### 3.4. Model preparation

For the sake of simplicity, two centrifugal tests were carried out with dry Toyoura sand with good engineering properties. This is a kind of fine sand with poor gradation, and the particle size ( $D_{50}$ ) is 0.17 mm. The maximum void ratio ( $e_{\max}$ ), minimum void ratio ( $e_{\min}$ ), specific gravity ( $G_s$ ) and internal friction angle ( $\varphi_c$ ) were 0.977, 0.597, 2.65 and  $31^\circ$ , respectively [25–27].

In this study, sand rain method was used to prepare relatively uniform and repeatable sand samples. In order to obtain medium density sand samples, the measured rainfall distance from the sand surface is maintained at 800 mm. When the sand reaches the inverted arch level of tunnel and pipeline, the model tunnels and pipelines are installed respectively. After the model preparation, the average dry densities of sand samples were 1490 and 1493 kg/m<sup>3</sup>, respectively. The relative densities ( $D_r$ ) of test 1 (continuous tunnel) and test 2 (joint tunnel) were 0.52 and 0.53, respectively.

### 3.5. Centrifuge testing procedures

After the centrifugal model was prepared, the gravity acceleration gradually increased from 1 g to 60 g. When all LVDT and strain gauge readings are stable, the tunnel excavation in the air is simulated by controlling well-drained water. The test is divided into five stages: the centrifuge acceleration rises to 60 g, after the measurement data reading is stable, the air valve is opened, and the liquid in the water belt is gradually released to simulate the tunneling process of the tunnel. After the zinc chloride solution in each water-saving bag is released, wait for 2 minutes and release the next section. As shown in Fig. 3a. The excavation process of the newly excavated tunnel is simulated by the method of discharging heavy liquid.

The excavation sequence is from 1L to 6R and 3L, 3R, 4L and 4R are below the constructed high-speed railway tunnel. The length of each excavation is 60 mm which correspond to site is 3.6 m. On the lower side of the model box is a reserved square slot for placing the control valves and heavy liquid storage tanks required to simulate tunnel excavation.

## 4. Three-dimensional numerical analysis

### 4.1. Model overview

To further study the influence of settlement joints and steel pipe pile on existing tunnels. The finite element software MIDAS/GTS is used to establish a three-dimensional numerical calculation model. The size of the model is  $120\text{ m} \times 120\text{ m} \times 80\text{ m}$ . The grid of the existing tunnel and the new tunnel is locally encrypted. The bottom of the model is completely constrained and the side is horizontally constrained. Three deformation joints are set along the longitudinal direction of the existing high-speed railway tunnel. The total number of grids is 450 thousands and the total number of node is 420 thousands. All deformation joints are filled with entities to restrict their longitudinal displacement. The buried depth of the existing high-speed railway tunnel is 4.3 m, and the tunnel structure is horseshoe section. The buried depth of the new tunnel is 29.6 m. The overall grid of the model is shown in Fig. 6a. The position relationship between the existing tunnel and the new tunnel is shown in Fig. 6b. The reinforced steel pipe pile is shown in Fig. 6c.

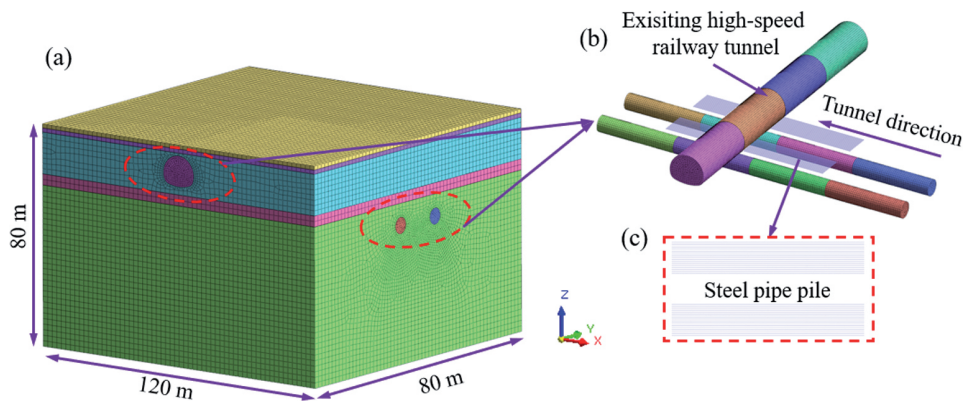


Fig. 6. Finite element calculation model: (a) overall calculation model; (b) the position relationship between the existing tunnel and the new tunnel; (c) steel pipe pile

### 4.2. Design conditions

The initial support of the existing high-speed railway tunnel is C35 concrete with a thickness of 35 cm, and the secondary lining is C40 concrete with a thickness of 40 cm. The newly-built shield tunnel adopts C50 concrete with segment diameter of 6 m and thickness of 30 cm. The lining of the existing tunnel, the segments of the new tunnel and the soil are simulated by solid element, and obey the Mohr-Coulomb yield criterion. Considering the influence of segment joint on lining strength, the elastic modulus of segment should be reduced by 20%. The structural physical parameters are shown in Table 2.

Table 2. Material properties of the structures

Materials	Unit weight (kN/m <sup>3</sup> )	Elastic modulus (MPa)	Poisson ratio
Secondary lining of high speed railway tunnel	25	$3.15 \times 10^4$	0.20
Invert filling concrete	25	$2.55 \times 10^4$	0.20
Concrete slab	25	$3.25 \times 10^4$	0.20
Segment lining	25	$2.76 \times 10^4$	0.20
Shield machine	78.5	$2.10 \times 10^5$	0.25

### 4.3. Construction process simulation

Due to the long distance of shield propulsion, alternate passivation of tunnel soil unit and activation of shield shell unit, segment unit and grouting layer are adopted to simulate the process of tunnel excavation and grouting reinforcement. The shield shell, grouting and other layers are simulated by plate element, and the grouting pressure is added at the same time. The cutting effect between the cutterhead and the soil is simulated by applying circumferential force on the soil surface. The simulation of excavation process mainly includes shield excavation, the application of earth pressure, torque, top thrust and grouting reinforcement. Considering that grouting reinforcement needs a process to form strength bearing, the grouting pressure and grouting layer are applied to simulate, and the segments are continuously applied with the advancement of shield machines.

In the whole excavation process, the main role of the shield is to support the surrounding soil, passivation shield is the shield tail away from the current position; the soil in the passive excavation area is excavated in the actual excavation process; activation segment is the segment assembly in the actual tunneling process; activation grouting is the shield tail grouting in the actual tunneling process, but the grouting has a curing process. Therefore, in the simulation construction process, after all the excavation is completed, the grouting layer is solidified and realized by changing the material properties. The simulation of shield tunneling process is shown in Fig. 7.

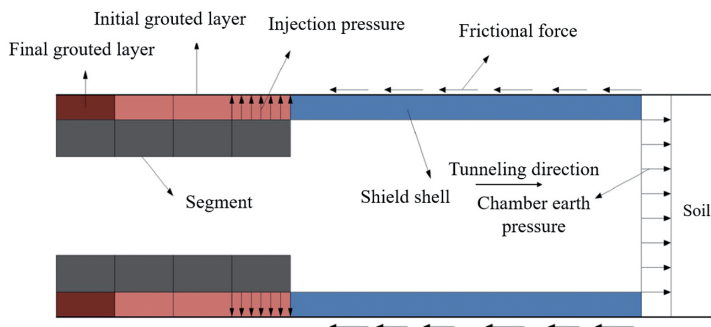


Fig. 7. Simulation of shield tunneling process

## 5. Results and discuss

### 5.1. Study on deformation law of shield tunneling under existing tunnel

Figure 8 is the vertical displacement nephogram of the existing tunnel when the double-line shield tunnel excavation is completed. It can be seen from Fig. 8 that after the excavation of the left tunnel, the maximum settlement value of the existing tunnel lining appears above the axis of the left tunnel, which is 1.73 mm; after the completion of the right line tunnel excavation, the settlement value distribution of the existing tunnel lining is small at both ends and large in the middle, and the maximum value is 2.56 mm. The settlement value of the existing tunnel caused by the first shield tunnel construction has reached 67% of the completion of the tunnel construction. It can be seen that the first shield tunnel has a great influence. In addition, shield tunnel excavation has a great influence on the lining of high-speed railway tunnel just above.

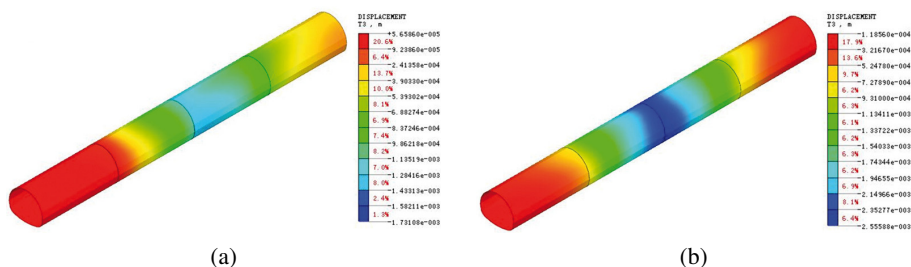


Fig. 8. Horizontal displacement changes of Liuyang River tunnel in different construction stages: (a) after excavation of 1st new tunnel; (b) after excavation of 2nd new tunnel

### 5.2. Longitudinal bending strain of existing tunnels induced by double tunnel excavation

Figure 9 shows the bending strain of the existing tunnel arch bottom caused by the double-track shield excavation. It can be seen from the diagram that the calculated value and the measured value are slightly different, which may be due to the assumption that the existing tunnel is calculated according to the theory of the beam, resulting in inaccurate. However, the calculated values of longitudinal bending strain are in good agreement with the measured values, and the maximum values are basically the same.

As shown in Fig. 9, the bending positive strain occurs on both sides of the middle line of the existing tunnel, and the bending negative strain is at both ends of the existing tunnel. The change is basically consistent with the settlement curve of the arch bottom. After the left and right line shield excavation is completed, the total bending strain in the middle of the existing tunnel is  $37.6 \mu\epsilon$ , and the negative strains at both ends are  $-9 \mu\epsilon$  and  $-5 \mu\epsilon$ , respectively. Considering that in ACI2001, the ultimate tensile strain (cracking) of unreinforced concrete is  $150 \mu\epsilon$ . In this test, the measured tensile strain is less than  $150 \mu\epsilon$ ,

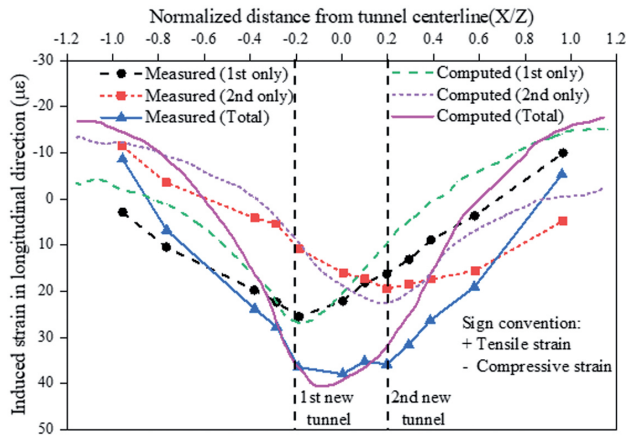


Fig. 9. Influence of double tunnel construction on longitudinal bending moment of existing tunnel

because the size and thickness of the existing tunnel is very large, resulting in a more general tunnel (the left and right lines in this test) stiffness is much larger.

The maximum bending strain caused by the excavation of the left line is  $25.2 \mu\epsilon$ , which appears on the axis of the left line and gradually changes to  $-8 \mu\epsilon$ . The maximum bending strain caused by right line excavation is 11% smaller than that caused by left line excavation. The arch bottom settlement and longitudinal bending strain results of the existing line caused by the above double-line excavation mean that the influence of the right line of subsequent excavation on the existing tunnel is smaller, which is basically 5÷11% smaller. The reason for this phenomenon is that after the left-line shield excavation is completed, the soil stress near the existing tunnel is redistributed. The first excavated left line reduces the soil stiffness in a small range near the excavated tunnel, because the constraint pressure near the tunnel is reduced. However, the stiffness of the adjacent soil is improved due to the increase of the constraint pressure, such as the soil near the existing tunnel and the subsequent excavation of the right-line tunnel, so the influence of the right-line excavation on the existing tunnel is smaller.

### 5.3. Study on stress law of shield tunnel undercrossing existing tunnel

Figure 10 shows the axial stress diagram at the vault of the existing tunnel lining with and without construction joints in the numerical model. The maximum tensile stress of the existing tunnel without construction joints is 0.53 MPa. However, considering the construction joint, the stress distribution of segment lining is lower than the results discussed above, and the maximum tensile stress in lining is reduced to 0.42 MPa, which is 21% lower than that without considering the construction joint. In addition, the tensile stress near the construction joint decreases rapidly. In this case, the existing tunnel structure is in a safe state during the construction of the double-track shield tunnel, and the lining of the existing high-speed railway tunnel is not damaged.

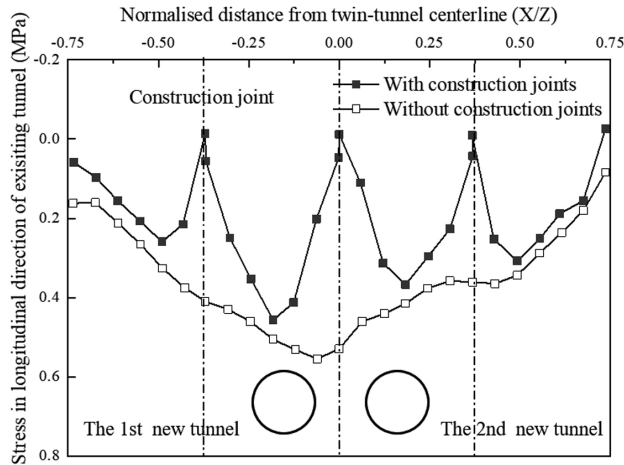


Fig. 10. Influence of double tunnel excavation on axial stress of existing tunnel

Fig. 11 shows the numerical results of circumferential stress of tunnel cross section when  $X/Z = 0$ .

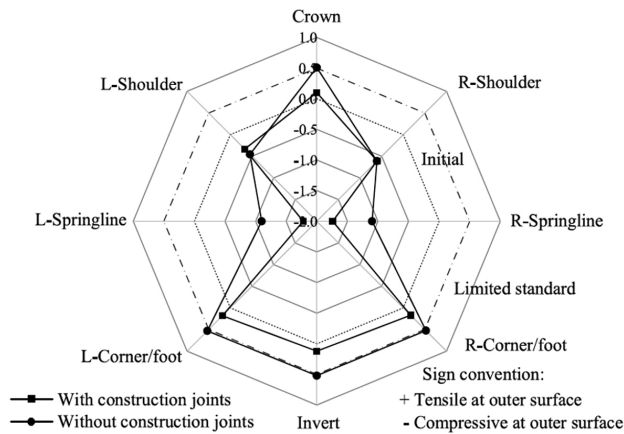


Fig. 11. Circumferential stress induced by excavation of new tunnels

The results show that the calculated tensile stress on the vault, invert and foot sides of the tunnel is consistent with the stress distribution in the centrifugal test. Without considering the construction joints, the maximum tensile stress is 0.53 MPa. On the contrary, considering the construction joint, the maximum tensile stress is 0.18 MPa. However, the mechanical performance shows that the existing tunnel is in a safe state considering the construction joints. The stress exceeds the actual stress without considering the construction joints, which may lead to more conservative construction measures.

### 5.4. Study on internal force law of shield tunnel undercrossing existing tunnel

Figures 12, 13 and 14 show the internal force contours of the lining of the high-speed railway tunnel before shield construction, after the completion of the right line excavation and after the completion of the left line excavation.

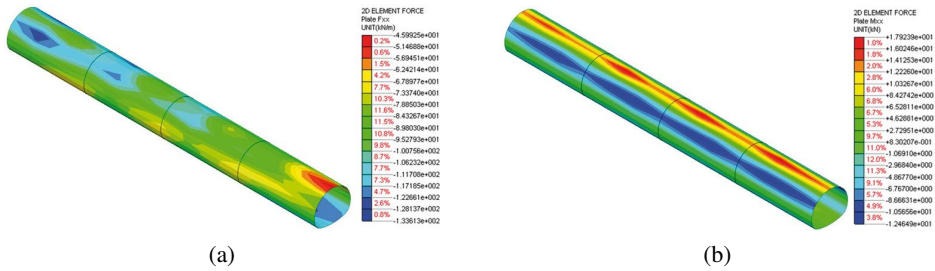


Fig. 12. Internal force diagram of existing tunnel before shield construction: (a) axial force diagram; (b) Moment diagram

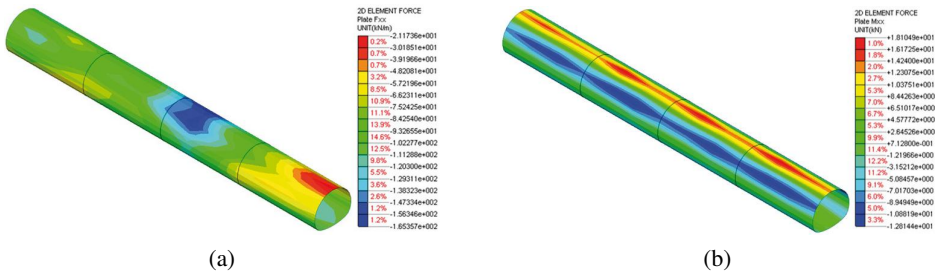


Fig. 13. The internal force diagram of the existing tunnel after the completion of the right line excavation: (a) axial force diagram; (b) Moment diagram

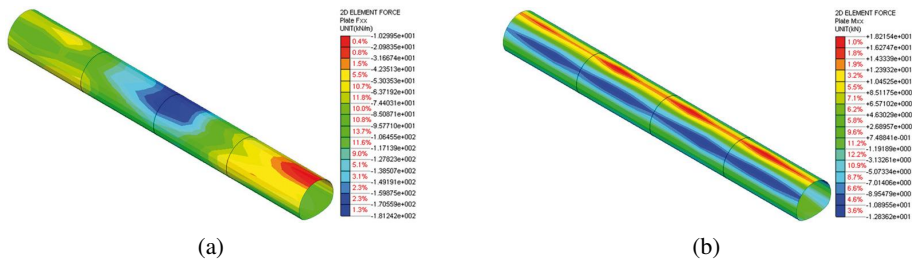


Fig. 14. The internal force diagram of the existing tunnel after the completion of the left line excavation: (a) axial force diagram; (b) Moment diagram

It can be seen from the figure that after the lining construction of the existing high-speed railway tunnel is completed, the lining axial force is concentrated at the bottom of the lining and the arch waist position, and the maximum axial force is 1336.1 kN. After the excavation of the right line of the shield, the axial force of the lining of the high-speed railway tunnel above the right line is concentrated at the vault, and the maximum stress concentration is 1653.6 kN; after the excavation of the left line of the shield, the axial force concentration area of the lining extends to the lining just above the left line. The axial force concentration area is located at the deformation joint of the lining, and the maximum axial force is 1812.4 kN, increasing by about 476.3 kN. The comparative analysis shows that shield excavation has a certain influence on the axial force change at the deformation joint of Liuyang River tunnel lining, and the increase is small, which is far less than the allowable bearing capacity of high-speed railway tunnel. According to the variation of bending moment of high-speed railway tunnel lining with shield excavation, it can be seen that the bending moment of lining does not appear concentrated at the joint of deformation joints. After the completion of high-speed railway tunnel construction, the maximum lining bending moment is 124.6 kN·m. After the excavation of the right line and the left line of the shield, the maximum lining bending moments are 128.1 kN·m and 128.4 kN·m, respectively. The comparative analysis shows that the bending moment of high-speed railway tunnel lining changes little after shield excavation, and the influence of shield excavation on high-speed railway tunnel lining is small.

### 5.5. Analysis of surface subsidence caused by shield excavation

Figure 15 is the surface subsidence curve caused by shield excavation in three different cases, three cases are: (a) set three subsidence joints along the high-speed railway tunnel and connect with the lining; (b) The settlement joint of the high-speed railway tunnel is not considered; (c) The influence of high-speed railway tunnel is not considered.

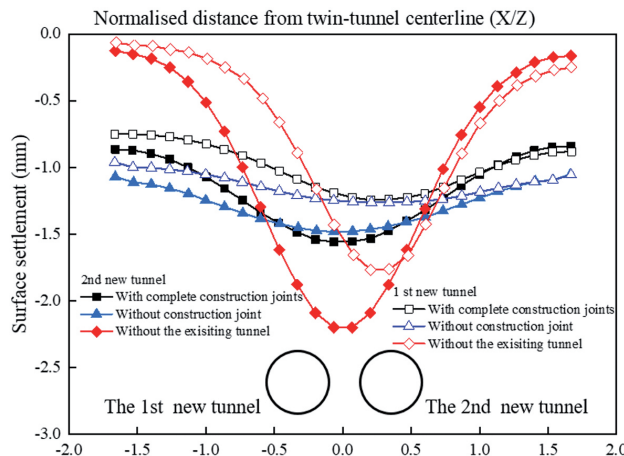


Fig. 15. Surface subsidence curve caused by double shield excavation

It can be seen from the diagram that when considering the construction joint of the existing high-speed railway tunnel, the width of the ground settlement trough is obviously larger than that without considering the construction joint. Although the depth of the ground settlement trough increases during the excavation of the right line tunnel, the research results still show that the settlement trough caused by the construction joint of the high-speed railway tunnel lining is relatively narrow but deeper than that without considering the construction joint. In addition, without considering the existing tunnel, the maximum ground settlement is 2.19 mm, 49% larger than that without construction joints and 41% larger than that with construction joints.

The above results show that the existence of construction joints will reduce the shielding effect of high-speed railway tunnel on surface settlement. Nevertheless, compared with the case without existing tunnels, the existing tunnels considering construction joints have obvious shielding effect on surface settlement. When ignoring the existence of existing tunnel construction joints, it will cause large settlement trough and underestimate the maximum settlement value.

### 5.6. Effect of steel pipe pile reinforcement on vertical displacement of existing tunnel

According to the existing high-speed railway tunnel control specification requirements [28], the maximum vertical settlement of the high-speed railway tunnel in operation should not be higher than 2 mm. Combined with Fig. 9, it can be found that the maximum settlement of the existing high-speed railway tunnel caused by the construction of the double-line shield tunnel is as high as 2.56 mm, which is beyond the maximum allowable range of the specification. This shows that the soil needs to be strengthened before the shield excavation to control the settlement of the existing high-speed railway tunnel. Fig. 16 is the displacement nephogram of the existing tunnel considering the reinforcement of steel pipe piles. It can be seen from the figure that the vertical displacement of the lining of the existing high-speed railway tunnel decreases significantly after the reinforcement of the steel pipe pile. When the right line tunnel construction is completed, the maximum settlement of the existing high-speed railway tunnel lining is 1.42 mm, and when the double

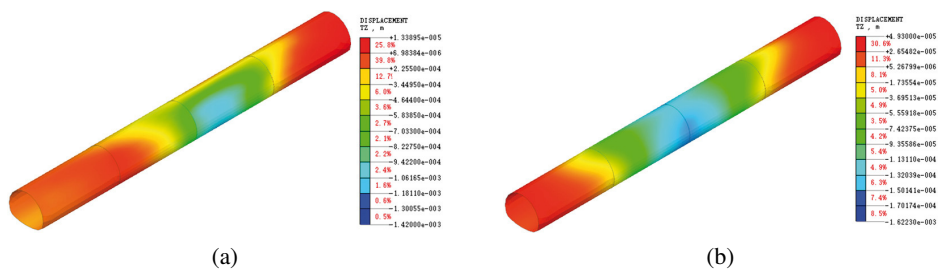


Fig. 16. Surface subsidence curve caused by double-line shield excavation (a) after excavation of 1st new tunnel; (b) after excavation of 2nd new tunnel

line shield tunnel construction is completed, the maximum settlement of the existing high-speed railway tunnel lining is 1.62 mm, which is within the safe range considered in the specification. That is to ensure the safe operation of the existing high-speed railway tunnel needs to consider the reinforcement of the steel pipe pile in the shield tunnel construction.

## 6. Conclusions

This paper studies the influence of new shield tunnel undercrossing on existing high-speed railway tunnel. Combined with centrifuge model test and three-dimensional numerical simulation analysis results, the following conclusions can be drawn:

1. A refined numerical model of existing tunnels considering construction joints is proposed. The results of numerical analysis show that the construction joints of existing tunnels significantly reduce the shielding effect of existing high-speed railway tunnels on the ground. Compared with the case without considering the construction joints, the smaller shielding effect leads to the increase of the vertical displacement of the existing tunnel and the surface. When the construction joints are considered in the existing tunnel, the maximum ground settlement increases and the width of settlement trough decreases.
2. The settlement value of the existing tunnel caused by double-line shield tunnel construction needs to be controlled by steel pipe pile reinforcement to meet the requirements of the specification. The double-line shield tunnel construction has little effect on the internal force of the existing high-speed railway tunnel, and the reinforcement of the high-speed railway tunnel lining meets the stress requirements.
3. The existence of construction joints changes the mechanical response of high-speed railway tunnel structure to the construction of double-line shield tunneling. The maximum stress of existing tunnel lining caused by double-line tunnel construction is reduced by the existence of construction joints, especially the tensile stress near the construction joints. In other words, without considering the construction joints, the numerical analysis underestimated the surface settlement, but overestimated the mechanical performance of the results of the existing tunnel.

At present, the soil is usually considered as a multi-layer uniform material, and the influence of groundwater level is usually ignored in the research process. In particular, the effective and accurate analysis in numerical simulation needs to further consider the influence of fluid-solid coupling effect on soil. The author will study it further in the future.

## Acknowledgements

This work was funded by the National Natural Science Foundation of China under Grant Nos. 51978669 and the China Railway Design Corporation Foundation under Grant Nos. 721239. The authors are grateful for the great support awarded.

## References

- [1] E. Deng, W.C. Yang, M.F. Lei, et al., “Instability mode analysis of surrounding rocks in tunnel blasting construction with thin bedrock roofs”, *Geotechnical and Geological Engineering*, vol. 36, pp. 2565–2576, 2018, DOI: [10.1007/s10706-018-0483-1](https://doi.org/10.1007/s10706-018-0483-1).
- [2] E. Deng, W.C. Yang, and P.P. Zhang, “Analysis of surrounding rock vibration and the influence of soft rock mechanical parameters during the tunnel blasting with thin bedrock roof”, *Geotechnical and Geological Engineering*, vol. 38, pp. 537–550, 2020, DOI: [10.1007/s10706-019-01044-3](https://doi.org/10.1007/s10706-019-01044-3).
- [3] J.S. Zhang and Y.Z. Qi, “Research on the intelligent positioning method of tunnel excavation face”, *Archives of Civil Engineering*, vol. 68, no. 1, pp. 431–441, 2022, DOI: [10.24425/ace.2022.140178](https://doi.org/10.24425/ace.2022.140178).
- [4] R.P. Chen, F.Y. Meng, Z.C. Li, et al., “Investigation of response of metro tunnels due to adjacent large excavation and protective measures in soft soils”, *Tunnelling and Underground Space Technology*, vol. 58, pp. 224–235, 2016, DOI: [10.1016/j.tust.2016.06.002](https://doi.org/10.1016/j.tust.2016.06.002).
- [5] B. Liu, D.W. Zhang, C. Yang, et al., “Long-term performance of metro tunnels induced by adjacent large deep excavation and protective measures in Nanjing silty clay”, *Tunnelling and Underground Space Technology*, vol. 95, art. no. 103147, 2020, DOI: [10.1016/j.tust.2019.103147](https://doi.org/10.1016/j.tust.2019.103147).
- [6] A. Siemińska-Lewandowska and, R. Kuszyk, “Study of subsiding trough expansion over twin tube TBM metro tunnel”, *Archives of Civil Engineering*, vol. 64, no. 4, pp. 119–133, 2018, DOI: [10.2478/ace-2018-0066](https://doi.org/10.2478/ace-2018-0066).
- [7] Z. Wang, K.W. Zhang, G. Wei, et al., “Field measurement analysis of the influence of double shield tunnel construction on reinforced bridge”, *Tunnelling and Underground Space Technology*, vol. 81, pp. 252–264, 2018, DOI: [10.1016/j.tust.2018.06.018](https://doi.org/10.1016/j.tust.2018.06.018).
- [8] Q. Fang, D.L. Zhang, Q.Q. Li, et al., “Effects of twin tunnels construction beneath existing shield-driven twin tunnels”, *Tunnelling and Underground Space Technology*, vol. 45, pp. 128–137, 2015, DOI: [10.1016/j.tust.2014.10.001](https://doi.org/10.1016/j.tust.2014.10.001).
- [9] C.Y. Gue, M.J. Wilcock, M.M. Alhaddad, et al., “Tunneling close beneath an existing tunnel in clay – perpendicular undercrossing”, *Géotechnique*, vol. 67, no. 9, pp. 795–807, 2017, DOI: [10.1680/jgeot.SIP17.P.117](https://doi.org/10.1680/jgeot.SIP17.P.117).
- [10] A. Klar, I. Dromy, and R. Linker, “Monitoring tunneling induced ground displacements using distributed fiber-optic sensing”, *Tunnelling and Underground Space Technology*, vol. 40, pp. 141–150, 2014, DOI: [10.1016/j.tust.2013.09.011](https://doi.org/10.1016/j.tust.2013.09.011).
- [11] V. Avgerinos, D.M. Potts, and J.R. Standing, “Numerical investigation of the effects of tunneling on existing tunnels”, *Géotechnique*, vol. 67, no. 9, pp. 808–822, 2017, DOI: [10.1680/jgeot.SIP17.P.103](https://doi.org/10.1680/jgeot.SIP17.P.103).
- [12] H. Chakeri, R. Hasanpour, M.A. Hindistan, et al., “Analysis of interaction between tunnels in soft ground by 3D numerical modeling”, *Bulletin of Engineering Geology and the Environment*, vol. 70, no. 3, pp. 439–448, 2011, DOI: [10.1007/s10064-010-0333-8](https://doi.org/10.1007/s10064-010-0333-8).
- [13] H.L. Liu, P. Li, and J.Y. Liu, “Numerical investigation of underlying tunnel heave during a new tunnel construction”, *Tunnelling and Underground Space Technology*, vol. 26, no. 2, pp. 276–283, 2011, DOI: [10.1016/j.tust.2010.10.002](https://doi.org/10.1016/j.tust.2010.10.002).
- [14] C.W.W. Ng, K.Y. Fong, and H.L. Liu, “The effects of existing horseshoe-shaped tunnel sizes on circular crossing tunnel interactions: Three-dimensional numerical analyses”, *Tunnelling and Underground Space Technology*, vol. 77, pp. 68–79, 2018, DOI: [10.1016/j.tust.2018.03.025](https://doi.org/10.1016/j.tust.2018.03.025).
- [15] M.L. Yin, H. Jiang, Y.S. Jiang, et al., “Effect of the excavation clearance of an under-crossing shield tunnel on existing shield tunnels”, *Tunnelling and Underground Space Technology*, vol. 78, pp. 245–258, 2018, DOI: [10.1016/j.tust.2018.04.034](https://doi.org/10.1016/j.tust.2018.04.034).
- [16] Z.G. Zhang and M.S. Huang, “Geotechnical influence on existing subway tunnels induced by multi-line tunneling in Shanghai soft soil”, *Computers and Geotechnics*, vol. 56, no. 3, pp. 121–132, 2014, DOI: [10.1016/j.compgeo.2013.11.008](https://doi.org/10.1016/j.compgeo.2013.11.008).
- [17] T. Boonyarak, and C.W.W. Ng, “Effects of construction sequence and cover depth on crossing-tunnel interaction”, *Canadian Geotechnical Journal*, vol. 52, no. 7, pp. 851–867, 2015, DOI: [10.1139/cgj-2014-0235](https://doi.org/10.1139/cgj-2014-0235).

- [18] G. W. Byun, D. G. Kim, and S. D. Lee, "Behavior of the ground in rectangularly crossed area due to tunnel excavation under the existing tunnel", *Tunnelling and Underground Space Technology*, vol. 21, no. 3–4, 2006, DOI: [10.1016/j.tust.2005.12.178](https://doi.org/10.1016/j.tust.2005.12.178).
- [19] L.C. Miao, F. Wang, C.W.W. Ng, et al., "Centrifugal model tests on excavation of twin parallel tunnels", *Chinese Journal of Geotechnical Engineering*, vol. 39, no. 2, pp. 373–379, 2017, DOI: [10.11779/CJGE201702023](https://doi.org/10.11779/CJGE201702023).
- [20] P. Li, S.J. Du, X.F. Ma, et al., "Centrifuge investigation into the effect of new shield tunneling on an existing underlying large-diameter tunnel", *Tunnelling and Underground Space Technology*, vol. 42, pp. 59–66, 2014, DOI: [10.1016/j.tust.2014.02.004](https://doi.org/10.1016/j.tust.2014.02.004).
- [21] C.W.W. Ng, T. Boonyarak, and D. Mašín, "Three-dimensional centrifuge and numerical modeling of the interaction between perpendicularly crossing tunnels", *Canadian Geotechnical Journal*, vol. 50, no. 9, pp. 935–946, 2013, DOI: [10.1139/cgj-2012-0445](https://doi.org/10.1139/cgj-2012-0445).
- [22] C.W.W. Ng, T. Boonyarak, and D. Mašín, "Effects of pillar depth and shielding on the interaction of crossing multitunnels", *Journal of Geotechnical and Geoenvironmental Engineering*, vol. 141, no. 6, 2015, DOI: [10.1061/\(ASCE\)GT.1943-5606.0001293](https://doi.org/10.1061/(ASCE)GT.1943-5606.0001293).
- [23] C. W. W. Ng, R. Wang, and T. Boonyarak, "A comparative study of the different responses of circular and horseshoe-shaped tunnels to an advancing tunnel underneath", *Géotechnique Letters*, vol. 6, no. 2, pp. 168–175, 2016, DOI: [10.1680/jgele.16.00001](https://doi.org/10.1680/jgele.16.00001).
- [24] W.D. Pan, Z.Y. Gao, C.L. Zheng, et al., "Analysis on the influence of cross tunnel construction on the deformation of the existing high-speed railway tunnel", *Geotechnical and Geological Engineering*, vol. 36, pp. 4001–4013, 2018, DOI: [10.1007/s10706-018-0553-4](https://doi.org/10.1007/s10706-018-0553-4).
- [25] K. Ishihara, "Liquefaction and flow failure during earthquakes", *Géotechnique*, vol. 43, no. 3, pp. 351–415, 1993, DOI: [10.1680/geot.1993.43.3.351](https://doi.org/10.1680/geot.1993.43.3.351).
- [26] J. W. Shi, J.Q. Wei, C.W.W. Ng, et al., "Stress transfer mechanisms and settlement of a floating pile due to adjacent multi-propped deep excavation in dry sand", *Computers and Geotechnics*, vol. 116, art. no. 103216, 2019, DOI: [10.1016/j.compgeo.2019.103216](https://doi.org/10.1016/j.compgeo.2019.103216).
- [27] J.W. Shi, Z.Z. Fu, and W.L. Guo, "Investigation of geometric effects on three-dimensional tunnel deformation mechanisms due to basement excavation", *Computers and Geotechnics*, vol. 106, pp. 108–116, 2019, DOI: [10.1016/j.compgeo.2018.10.019](https://doi.org/10.1016/j.compgeo.2018.10.019).
- [28] MRPRC, *Standard for constructional quality acceptance of high speed railway track engineering (TB 10754-2018)*. Ministry of Railways of the People's Republic of China, 2018.

Received: 2022-08-23, Revised: 2022-11-08